DETAILED SPECIFICATION OF THE ARCTIC IONOSPHERE AND AN APPLICATION TO THREE-DIMENSIONAL RAYTRACING

J. Buchau, et al

Air Force Cambridge Research Laboratories
L. G. Hanscom Field, Massachusetts

27 November 1973

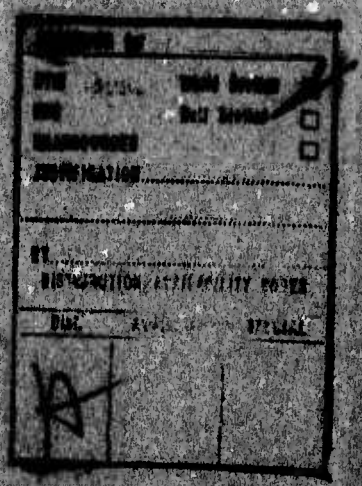

Unclassified
Security Classification

AD 775084

DOCUMENT CONTROL DATA - R&D

(Security classification of title, body of abstract and indexing annotation must be entered when the overall report is classified)

1. ORIGINATING ACTIVITY *(Corporate author)*
Air Force Cambridge Research Laboratories (LIB)
L.G. Hanscom Field
Bedford, Massachusetts 01730

2a. REPORT SECURITY CLASSIFICATION
Unclassified

2b. GROUP

3. REPORT TITLE
DETAILED SPECIFICATION OF THE ARCTIC IONOSPHERE AND AN APPLICATION TO THREE-DIMENSIONAL RAYTRACING

4. DESCRIPTIVE NOTES *(Type of report and inclusive dates)*
Scientific. Interim.

5. AUTHOR(S) *(First name, middle initial, last name)*
J. Buchau
C. P. Pike
M. Wong

6. REPORT DATE	7a. TOTAL NO. OF PAGES	7b. NO. OF REFS
27 November 1973	27	17

8a. CONTRACT OR GRANT NO.	9a. ORIGINATOR'S REPORT NUMBER(S)
b. PROJECT, TASK, WORK UNIT NOS. 5631-14-02	AFCRL-TR-73-0726
c. DOD ELEMENT 61102F	9b. OTHER REPORT NO(S) *(Any other numbers that may be assigned this report)* AFSG No. 279
d. DOD SUBELEMENT 681310	

10. DISTRIBUTION STATEMENT
Approved for public release; distribution unlimited.

11. SUPPLEMENTARY NOTES	12. SPONSORING MILITARY ACTIVITY
Paper Presented in the OHD Review Meeting, Air Force Academy, Colorado Springs, Colorado 2-3 May 1973	Air Force Cambridge Research Laboratories (LIB) L.G. Hanscom Field Bedford, Massachusetts 01730

13. ABSTRACT

A statistical analysis of Alouette topside ionograms shows that the probability of occurrence of the midlatitude F-layer trough is 100 percent in winter and at equinox, and is 50 percent in summer. The trough, which is generally centered on 55° corrected geomagnetic latitude and which is about 5° to 10° wide, extends throughout the night hemisphere with f_0F2 values less than 2 MHz.

Comparison of the location of the trough to the area in which coverage by an over the horizon backscatter (OTHB) system is anticipated shows that the trough will adversely affect system performance in the northeast direction most of the night. An in-depth case study of the effects of the trough on HF propagation was made, based on an instantaneous three-dimensional description of the ionosphere. This description of the ionosphere was composed of cross sections showing ionospheric electron-density structure in the area northeast of the Polar Fox II site. Three-dimensional raytracing was applied to this description of the ionosphere, and the trough and the steep electron-density gradient at the poleward edge of the trough were found to adversely affect propagation of HF signals. For 5 MHz, deviations from the initial azimuth were found to be as big as 15° (or 400 km distance to the great circle of initial azimuth) for rays landing at the skip distance. The deviations decrease with increase in frequency to 8 or 9 MHz, but here propagation depends on rays with low elevation angles (<5°).

DD FORM 1 NOV 68 1473

Unclassified
Security Classification

14. KEY WORDS	LINK A		LINK B		LINK C	
	ROLE	WT	ROLE	WT	ROLE	WT
Three-dimensional raytracing						
Polar Fox II						
Arctic radio propagation						
Over the horizon backscatter (OTH)						

Preface

We would like to thank Dr. G. J. Gassmann for his strong support of this work and for helpful discussions. Drs. K. Toman and T. Elkins supported the ray-tracing efforts. Drs. K. S. Vanguri and M. P. Friedman of Arcon, Inc., Wakefield, Massachusetts programmed the electron-density subroutine and the preprocessing programs.

Contents

Illustrations

Detailed Specification of the Arctic Ionosphere and an Application to Three-Dimensional Raytracing

1. INTRODUCTION

Some OTH backscatter systems in the planning stage or in an experimental test phase deal with a propagation environment quite different from that found in moderate zones—namely, the arctic ionosphere with all its irregular structure and rapidly varying behavior. Airborne investigation by AFCRL has shown that the arctic ionosphere, in spite of its complexity, exhibits a large-scale organization of a variety of ionospheric features that are either collocated with or parallel to the auroral oval. The auroral-oval concept provides the framework for ordering arctic ionospheric phenomena. In fact, the organization of the arctic ionosphere is now well enough understood that an analog model of the arctic ionosphere has been developed.[1, 2]

Figure 1 shows an electron-density cross section, constructed by Gassmann,[3] depicting the present, generalized concept of the structure of the arctic ionosphere

(Received for publication 26 November 1973)

1. Gassmann, G. J. (1972) An Ionospheric Model for the Arctic, Environmental Research Paper, No. 332, AFCRL-70-0562.

2. Gassmann, G. J. (1973) Analog Model 1972 of the Arctic Ionosphere, preprint, to be published as an AFCRL Report (February 1973).

3. Gassmann, G. J. (1972) High-latitude ionosphere, McGraw-Hill Yearbook of Science and Technology, McGraw-Hill Book Co., New York, pp. 257-260.

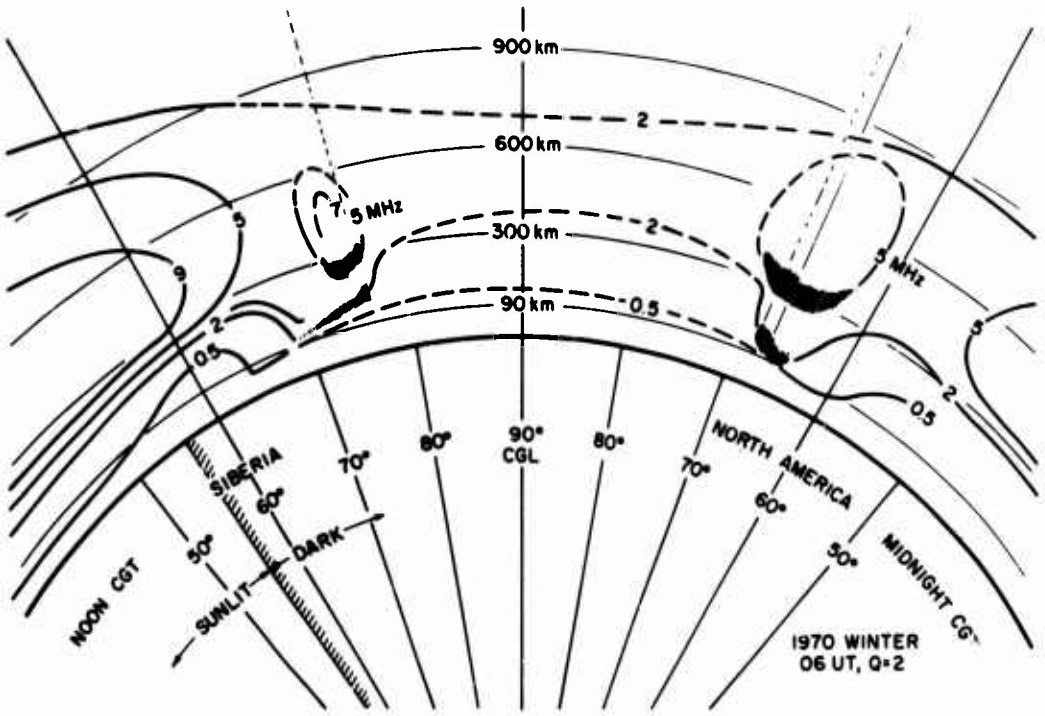

Figure 1. Noon-To-Midnight Cross Section of the Arctic Ionosphere

at solar maximum. The cross section applies to the noon-midnight meridian plane along approximately 80°W and 100°E. Along this meridian plane, in midwinter, the noon sector of the auroral oval is in darkness due to the tilt of the magnetic axis of the earth with respect to the rotational axis of the earth. This cross section shows circumpolar continuity of certain ionospheric features, for example, the auroral E layer[4] and the midlatitude F-layer trough.[5] These features are more pronounced in darkness than in sunlight when they are obscured by solar-produced ionization.

In this cross section, starting from the right, the end of the midlatitude nighttime F layer is seen, sharply bounded in the north by an approximately 10°-wide trough in which f_oF2 values are typically ≤ 2 MHz. The trough is terminated in

4. Wagner, R.A., and Pike, C.P. (1972) A discussion of arctic ionograms, AGARD Conf. Proc. 97, Frihagen, ed; pp. 4-1 to 4-20.

5. Muldrew, D.B. (1965) F-layer ionization troughs deduced from Alouette data, J. Geophys. Res. 70:2635-2650.

the north by the plasma-ring F-layer ionosphere[6] and by the auroral E layer.[4] These features are produced by a spatially continuous precipitation of 0.1- to 3-keV electrons. The typical critical frequency of the plasma ring in the vicinity of the poleward trough wall is 4 MHz. For the auroral E layer extending north from the poleward trough wall, 3 MHz f_0E is typical. Several degrees north of the poleward trough wall, F-region densities become somewhat enhanced, with f_0F2 values of 6 to 7 MHz. Large-scale irregularity structure is present, which gives this region its name: F-layer irregularity zone (FLIZ).[7,8] North of the FLIZ, the polar-cap f_0F2 values are approximately 2 MHz. The polar cap exhibits very strong but rather sporadic E- and F-region irregularities, which are probably associated with the occurrence of polar-cap aurora. At times the polar cap has low electron-density levels; hence, a polar cavity. In the noon sector, equatorward of the polar cap, there is a north-to-south sequence of F-, E-, and D-region ionization bands[9] produced by particle precipitation. If the noon sector is in darkness, as shown here, then the small depletion of electron density in this area indicates the location of the trough. Finally, the picture is terminated on the left by the northern edge of the noontime midlatitude F region.

2. STATISTICAL STUDY

Airborne observations have determined the general morphology of the F-region features.[4,9,10] To study in detail the dependence of these features on Kp, UT, season, solar cycle, and local time, the large data base resulting from the Alouette topside ionogram analysis was statistically investigated. The topside ionograms were routinely scaled for f_0F2 values by the Communications Research Centre, Ottawa, Canada. The f_0F2 data from 1962 to 1968 are contained on magnetic tapes, and CRC kindly provided copies of these tapes to AFCRL for special processing. This processing basically consisted of transforming the geographic

6. Andrews, M.K., and Thomas, J.O. (1969) Electron density distribution above the winter pole, Nature 221:223.

7. Pike, C.P. (1971) A latitudinal survey of the daytime polar F-layers, J. Geophys. Res. 76(No. 31):7745-7553.

8. Pike, C.P. (1972) Equatorward shift of the polar F-layer irregularity zone as a function of the Kp index, J. Geophys. Res. 77(No. 34):6911-6915.

9. Whalen, J.A., Buchau, J., and Wagner, R.A. (1971) Airborne ionospheric and optical measurements of noontime aurora, J. Atmos. Terr. Phys. 33 (No. 4):661-678.

10. Buchau, J., Gassman, G.J., Pike, C.P., Wagner, R.A., and Whalen, J.A. (1972) Precipitation patterns in the arctic ionosphere determined from airborne observations, Ann. Geophys. (Paris) 28(No. 2):443-453.

latitude and longitude of the satellite's position to corrected geomagnetic latitude (CGL) and corrected geomagnetic local time (CGLT),[11,12] enabling a statistical handling of the Alouette f_0F2 values in corrected geomagnetic coordinates rather than in geographic coordinates. This approach was selected because the high-latitude ionosphere is geomagnetically ordered. The geographic coordinates where the Alouette satellite recorded an ionogram were transformed to CGL and CGLT. The f_0F2 data were then divided into categories that should reflect the various dependencies. Alouette data from both northern and southern hemispheres were included in this study. Median f_0F2 values were taken over a 5° range of CGL and a 1-hr range of CGLT. Isocontours of f_0F2 median values were then drawn, and Figure 2 is a representative example of these isocontour maps. The basic map grid is CGL and CGLT. The contour lines are in 1-MHz increments except for the 1.5-MHz contour. The hatched area of median $f_0F2 \leq 2$ MHz is the statistical location of the trough with a core of $f_0F2 \leq 1.5$ MHz. The center of the trough is found between 55° and 60° CGL, moving slightly south to 55° for Kp > 1+. The trough width is generally greater than 10°. The polar cavity (low f_0F2 values) is seen in the vicinity of the magnetic pole. The two ionization tongues, which reach from evening and from morning toward the midnight sector, are the statistical average of the FLIZ. Due to the heavy spread-F conditions in the FLIZ, the actual maximum plasma frequencies of large-scale irregularities are not scaled, and the 1-MHz enhancement at the trough wall, noted here, shows only that the f_0F2 is enhanced poleward of the trough. Further evidence for the existence of a circumpolar FLIZ is the closed 3-MHz contour, located at 75° CGL in the 0900 CGLT sector, and the 3- and 4-MHz contours extending toward the 1800 CGLT sector.

Past studies of the effects of the arctic ionosphere on OTH and other radar systems, conducted by AFCRL,[13] have shown that strong horizontal electron-density gradients, found at the poleward trough wall, and low electron densities, found in the trough, strongly affect design parameters and performance of any planned system. Looking again at this general problem, the situation of an OTHB system assumed to be located at the POLAR FOX II site was considered.

---

11. Hakura, Y. (1965) Tables and maps of geomagnetic coordinates corrected by the higher order spherical harmonic terms, Rep. Ionosph. Space Res. (Japan) 19:121-157.

12. Whalen, J.A. (1970) Auroral Oval Plotter and Nomograph for Determining Corrected Geomagnetic Local Time, Latitude, and Longitude in the Northern Hemisphere, AFCRL-70-0422, Environmental Research Paper No. 327, Bedford, Mass.

13. Evans, D.L. (1971) Comp., Ionospheric and tropospheric limitations to radar accuracy, Air Force Surveys in Geophysics, No. 231, AFCRL-71-0169.

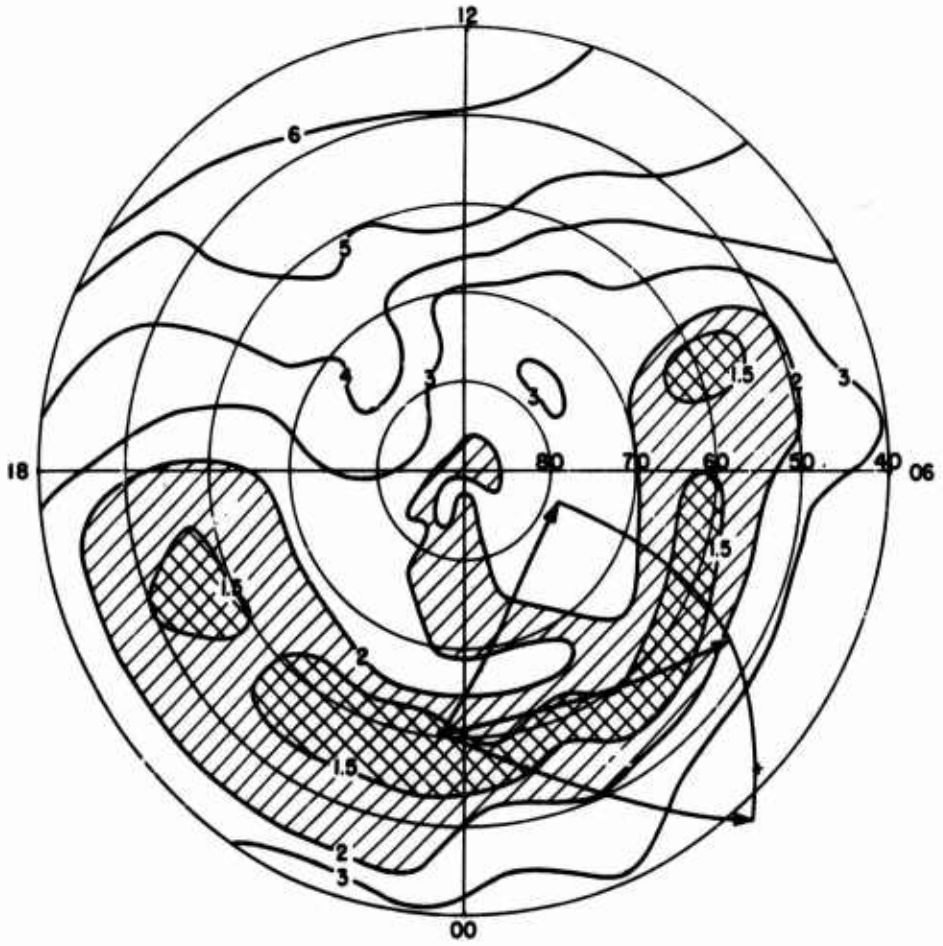

Figure 2. Contours of Median f_0F2 (in MHz) Derived From Alouette 1 Topside Soundings. Data base: Winter 1963, 0000 to 1200 UT, k_p 0 to 1+. The coordinate system is corrected geomagnetic latitude and corrected geomagnetic local time

The radar beam has been directed toward the northeast and has an azimuth range of ± 45°. The area of coverage of this radar beam has been converted into the CG coordinate system and is superimposed on the f_0F2 contour map in Figure 2. This presentation clearly points out that the boresight is aligned with the center of the trough, and the situation does not improve for southerly directions. Transmission toward the north will encounter the poleward trough wall and the FLIZ, and will therefore be strongly affected by auroral activity.

The actual situation of strong north-south electron-density gradients is not adequately represented by this averaged picture. The steepest gradients found in the statistical analysis were about 0.5 MHz per 100 km. The actual gradients,

determined from ground-based measurements[14] and airborne measurements[4] are approximately 2 to 3 MHz per 100 km.[15]

The probability of occurrence of f_0F2 values ≤ 2 MHz was then determined (Figure 3). Based on 1963 (solar minimum) data and on 1968 (solar maximum) data, the trough is present about 90 percent of the time in the winter and at equinox with a 100 percent probability of occurrence near midnight. The probability of occurrence of the trough drops to 50 percent in summer. The local-time extent of the trough has a strong seasonal dependence due to the change in solar illumination. The trough extends for approximately 12 hr and is centered on 01 CGLT in winter, extends for 6 to 8 hr at equinox and is centered on 02 CGLT, and extends in summer for less than 6 hr and is centered on 03 CGLT. Further study of the variability and the dependencies of the trough is still in progress. In this paper, effects of the trough on propagation will be discussed for a specific case study.

The statistical picture has shown that any OTHB system planned to operate at these latitudes will have to contend with the trough ionosphere. Therefore, an attempt was made to specify a large portion of the arctic ionosphere that could then be applied to an OTH situation. This was done for two reasons. First, we wanted to show by a well-documented example that median f_0F2 contour maps need interpretation because of the steep gradients that exist in reality. Second, we wanted to provide the input data for a three-dimensional raytracing program and to clearly show the effects of trough and strong north-south gradients on OTH propagation.

3. IONOSPHERIC SPECIFICATION

On 9 December 1971, a coordinated data-acquisition program involving aircraft, satellite, and ground stations provided a detailed picture of the ionosphere in the area north and east from the POLAR FOX II radar site. Airborne, satellite-borne, and ground-based ionosondes measured electron-density profiles, and from these measurements the trough, the steep electron-density gradient poleward of the trough, and the auroral ionosphere could be specified. In addition, unique new data that specified auroral conditions over a vast area were used.

---

14. Bowman, G. G. (1969) Ionization troughs below the F2-layer maximum, Planet. Space Sci. 17:777-796.

15. Buchau, J. (1972) Instantaneous versus averaged ionosphere, from "Arctic Ionosphere Modeling–Five Related Papers", Air Force Surveys in Geophysics, No. 241, AFCRL-72-0305.

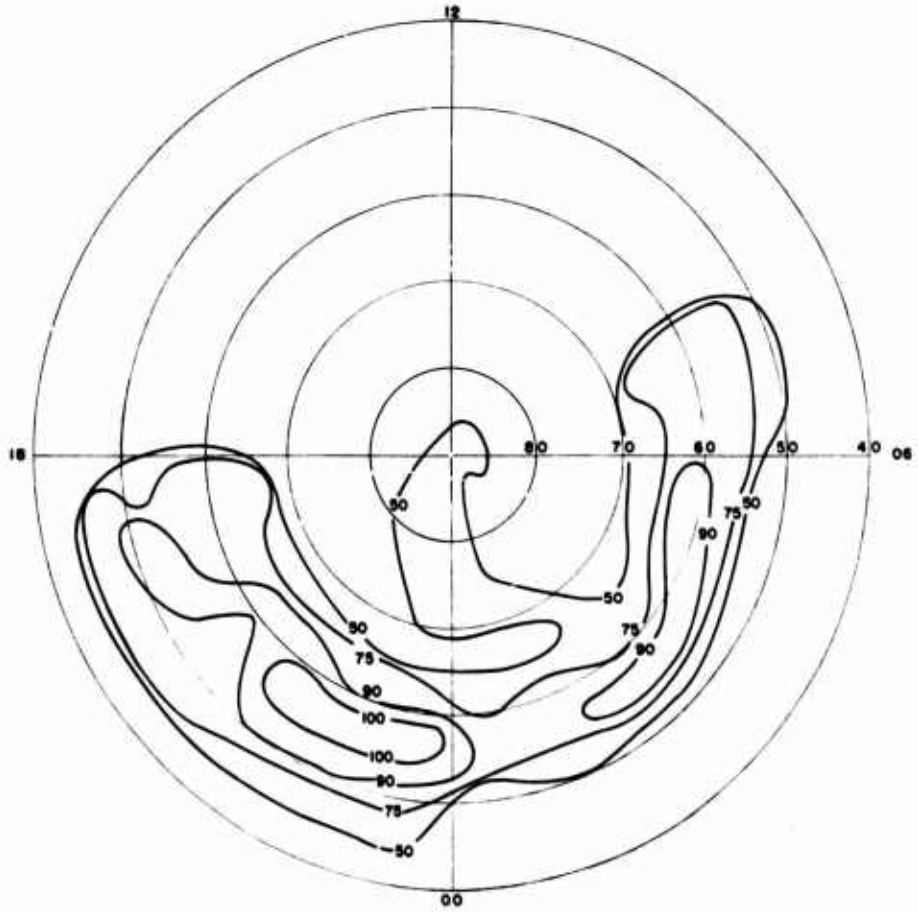

Figure 3. Contours of Percentage Occurrence of $f_0F2 < 2$ MHz. Data base and coordinate system same as Figure 2

These data are collected by a scanning photometer on board a satellite. An example of these new data is presented in Figure 4. This picture covers the eastern half of the United States and Canada and a major part of the Atlantic Ocean, including Greenland and the Arctic Ocean up to the North Pole. Of specific interest in the picture is an east-to-west-oriented belt of continuous aurora extending from Central Canada to Greenland. Near the poleward edge of the continuous aurora, discrete auroral arcs are seen.

The band of continuous aurora results from excitation of the arctic atmosphere by electron precipitation. The ionization that results from this precipitation produces the auroral-E layer, which is closely associated with the continuous aurora and the auroral-F layer. The poleward trough wall is approximately collocated with the equatorward edge of the continuous aurora. In this picture, moonlight

Figure 4. Satellite Picture Produced by Scanning Photometer, Showing Midnight Sector of Auroral Oval. A broadband of continuous aurora is bounded in the north and partially in the south by discrete aurora. Geographic features indicate dimensions of the coverage area

reflecting from clouds occurs in the east. By relating the location of auroral structure present in the picture to electron-density levels and gradients measured by ionosondes and the ISIS 2 topside sounder, a large-scale and accurate specification of the ionosphere could be inferred over the area of the picture in which no ionosonde data were recorded. In addition, by relating the location of auroral structures to the location of the radar site, the exact range from the site to the location where auroral effects would be expected to affect propagation conditions was read directly from the picture. Hence, a specification of the ionosphere and of HF propagation conditions of unprecedented dimensions has been achieved. These large-scale pictures of auroral conditions should, in general, be made available on a near-real-time basis to any system that may be affected by the ionosphere or by the aurora. By utilizing these pictures and routine frequency predictions, an accurate estimate of propagation conditions in close to real time could be reached.

A radar-beam position, directed northeast (45° east of north) from the POLAR FOX II site, was selected as the center line of a 76° sector in which a three-dimensional picture of the ionosphere was constructed. The sector is noted in Figure 5 as the area between the dashed lines. The northern hemisphere has been drawn in corrected geomagnetic coordinates. The central-beam position is labeled 0°, and beam positions ± 38.0° from the central-beam position are also noted.

Shading corresponds to the location of the continuous aurora seen in Figure 4. In the azimuth sector -6° to +6° with respect to the selected boresight (45° east of north), electron-density cross sections were provided in 2° increments (seven cross sections). The remaining sector between -38° and +38° was described every 4° in azimuth. Selected electron-density cross sections representative of the total of 25 cross sections produced are given in Figure 6. The -34° cross section (top of the figure) is a south-to-north cut through the polar ionosphere similar to the generalized presentation shown in Figure 1. The -4° and 0° cross sections just skim the poleward trough wall, showing sections of the trough ionosphere to the south of it.

The ionosphere south of the poleward trough wall is shown in the +34° cross section. It is in general a 2-MHz ionosphere with a narrow region of 1.5-MHz f_0F2. This trough ionosphere fluctuates in height between 360 and 470 km, which are the values taken from the ISIS 2 topside soundings of the 0420 UT pass that went exactly over the POLAR FOX II site, the origin of these cross sections.

In these cross sections the poleward trough wall is characterized by an abrupt increase in plasma frequency from 2 MHz in the trough to 4 MHz in the auroral F-layer or plasma ring. The FLIZ is seen in the -34° cross section as a 5-MHz

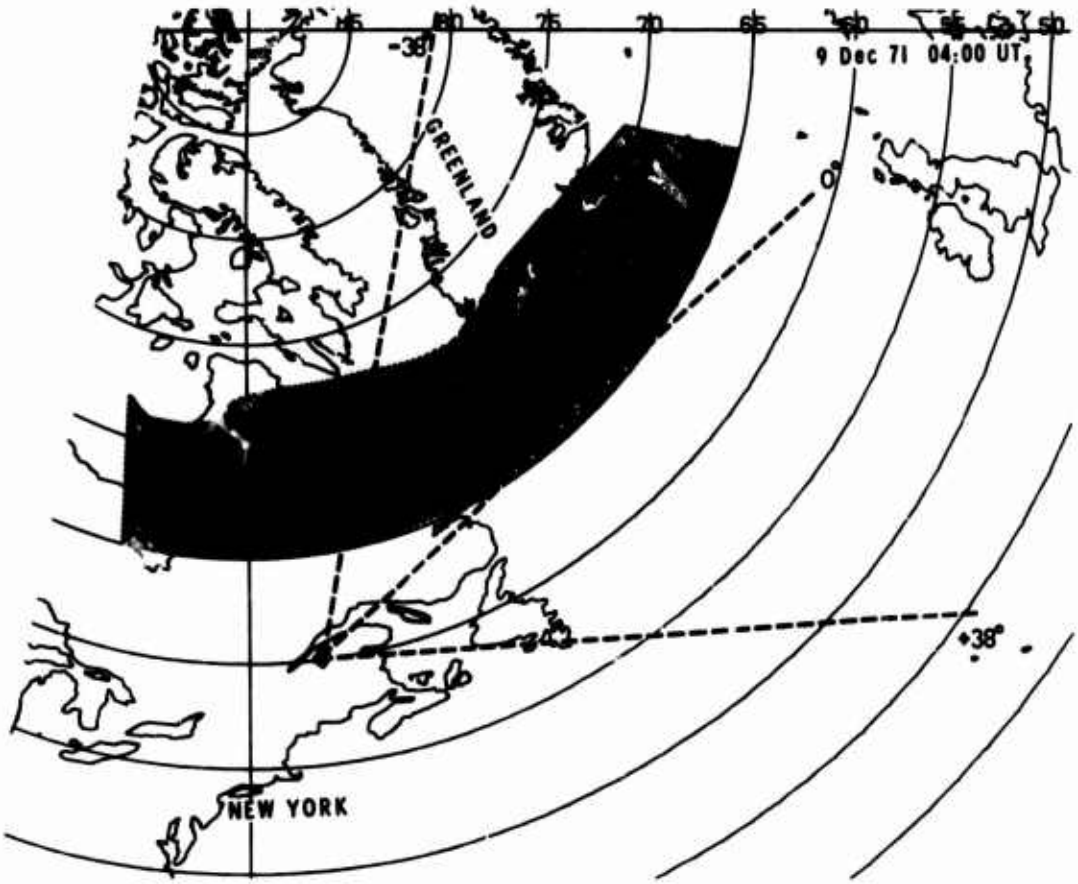

Figure 5. Continuous Aurora Shown in Figure 4 Transferred into the Corrected Geomagnetic Coordinate System. Note extremely good representation of the aurora midnight sector in corrected geomagnetic coordinates. Black square indicates location of POLAR FOX II. The sector of the ionosphere studied lies between -38° and +38° azimuth with respect to the 0° boresight in 25 radial cross sections

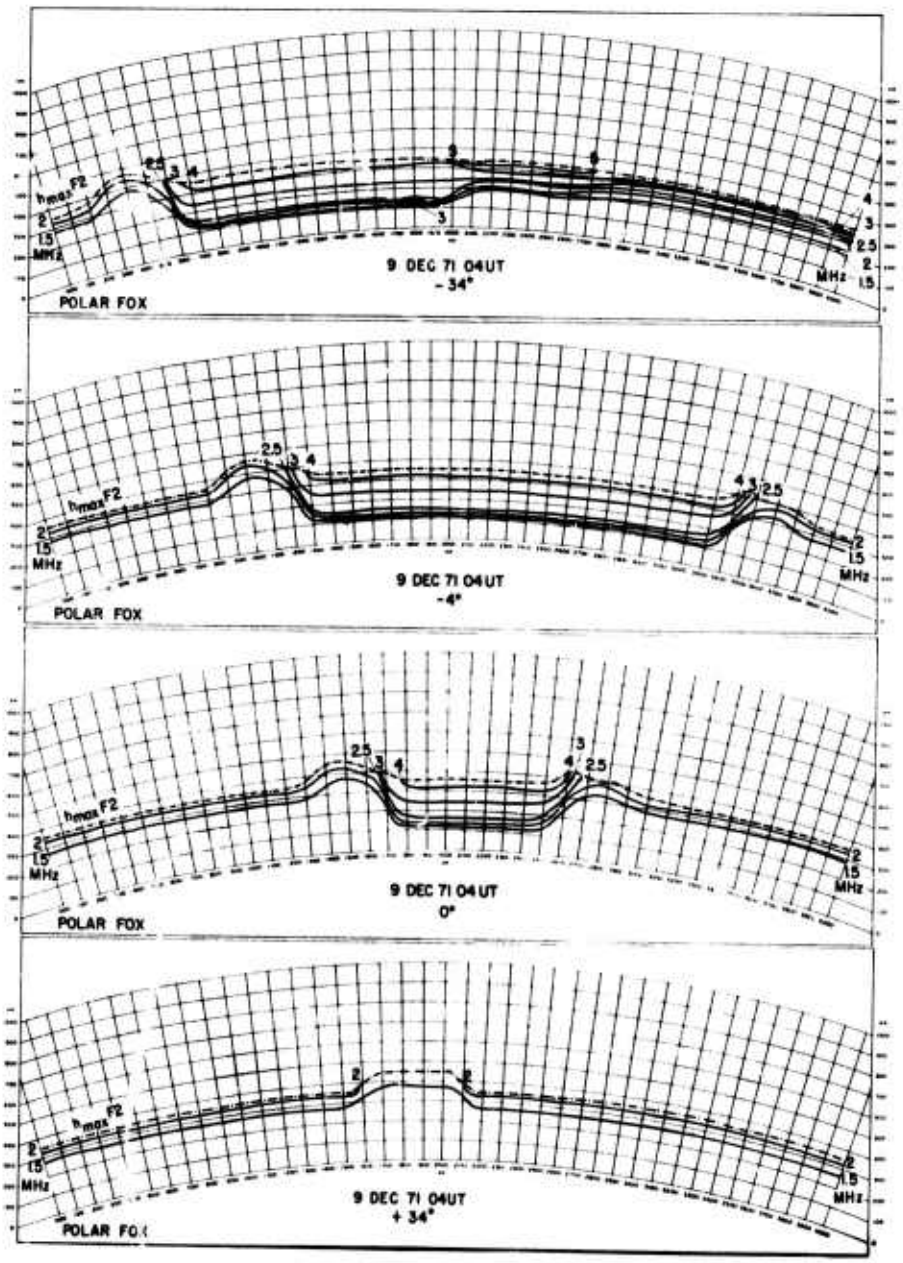

Figure 6. Four Typical Examples of Ionospheric Cross Sections

enhancement north of the aurora. The aurora itself is represented as an auroral Es with ftE_sa about 3 to 4 MHz at 1800 km distance from the POLAR FOX II site in the -34° azimuth.

The strong horizontal gradients of 2 to 3 MHz per 100 km found in the vicinity of the poleward trough wall by Bowman[14] and Wagner and Pike[4] are definitely present in this case study of 9 December 1971. In order to study the effects on radio wave propagation of this specific, but (from our experience, for this location and time) rather typical ionosphere, the cross sections were used as an input to a three-dimensional raytracing program.

4. RAYTRACING

In a first raytracing attempt a spherical-coordinate system was positioned with its pole at the radar site. Seven ionospheric cross sections (± 6°, ± 4°, ± 2°, and 0° with respect to a boresight of 45° east of north) were used as the meridional planes of this coordinate system. Since it turned out that the deviation of the computed rays was greater than the described ionosphere allowed for, the ionosphere was described by a total of 25 cross sections in an azimuth range ± 38° from boresight. This ionosphere was transformed into the geomagnetic dipole system for a second raytracing attempt. Both chosen coordinate systems are spherical, so that all parts except the electron-density subroutine of the highly regarded Jones raytracing program[16] can be used for our purpose. The dipolar coordinates are not as desirable as the corrected geomagnetic coordinates, but are a considerable improvement over the geographic coordinates for simulation of electron distributions in the polar ionosphere. In particular the boundary of the trough is nearly constant in corrected geomagnetic latitude, and extends over an interval of several degrees in dipolar latitude but tens of degrees in geographic latitude. The selection of a coordinate system that better orders the ionospheric features simplifies and improves the interpolation between two meridional planes.

AFCRL has developed an electron-density subprogram and incorporated it into the Jones raytracing program. Input data to this subprogram consist of plasma-frequency values specified at uniform grid-size intervals of r, θ, and ϕ; in the present study, intervals of 4 km in height, 0.5° dipolar latitude, and 5° in longitude were used. The output of this subprogram, feeding into the Jones raytracing program, provides values of the plasma frequency and its spatial derivatives at fine-step intervals (determined by integration step size) along the raypath.

16. Jones, R. M. (1968) A three-dimensional raytracing computer program, Radio Science 3(No. 1):93-94.

The input to the electron-density subprogram comes from an external preprocessing program. The input to the preprocessing program consists of the loci of plasma-frequency contours in each of a number of vertical meridional planes of the coordinate system used. Meridional planes, and data points in each plasma-frequency contour, are chosen at all locations where significant changes occur in the principal features (such as the trough and plasma ring) of the electron distribution.

Within the preprocessing program, a particular mode of interpolation introduced at AFCRL[17] is used in order to ensure that a principal feature that appears in each of two chosen meridional planes would be projected as one and only one principal feature at all intermediate planes between the two chosen ones. If this stipulation were not fulfilled, incorrect horizontal gradients of the electron-density (hence incorrect off-great-circle deviation of raypaths) would be obtained at some portions of the raypaths. Within the electron-density subprogram of the raytracing program, ordinary interpolation is used. Hence, at the level of fine coordinate increments (4 km in height, 0.5° in θ, and 5° in ϕ for the present study), residual and extraneous errors in horizontal gradients of electron-density still occur; however, these residual errors would cause only random fluctuations in the off-great-circle deviations of raypaths.

The principal drawback of the method of simulating electron-density distributions described above is the large size of the central memory required in the central processor of the computer system. A central-memory size of 260,000 (in the octal-number system) was used, approximately 200,000 for numerical data, and 50,000 for the Jones raytracing program.

There are two chief advantages of the method: raytracing speed, and a do-it-yourself capability for the raytracing user. It takes approximately 0.7 sec of computing time with the CDC-6600 computer to compute a one-hop, 3000-km raypath. The user can easily visualize the simulated electron-density distribution that is actually introduced into the raytracing computations, and retains assurance that the electron-density would be well approximated at the data-grid points and also that there would be no wild or unintended fluctuations of electron-density between grid points. The so-called problem of control or instability, troublesome in analytical representations of electron-density involving summation of a large number of terms (each a product of functions of r, θ, and ϕ), is bypassed in the method used here.

17. Wong, M.S. (1973) AFCRL Report to be published.

5. RAYTRACING RESULTS

Figure 7 shows as an example the results of the raytracing for 6 MHz, starting with an initial azimuth of -1° relative to the chosen boresight of 45° east of north. The upper part shows a projection of the raypaths into the meridional plane of the initial azimuth while the lower part shows the deviations from the initial azimuth in a projection into the horizontal plane, given here in range and azimuth. A group of curves allows one to judge the distance of the landing points of a ray to the great circle of the initial azimuth. The following figures will show only the heavy line connecting the landing points in Figure 7 as the most relevant result of the raytracing. Raytracing was done for 5, 6, 7, 8, and 9 MHz for initial azimuths of +5 to -9° (in 1° increments) with respect to the 0° reference (45° east of north).

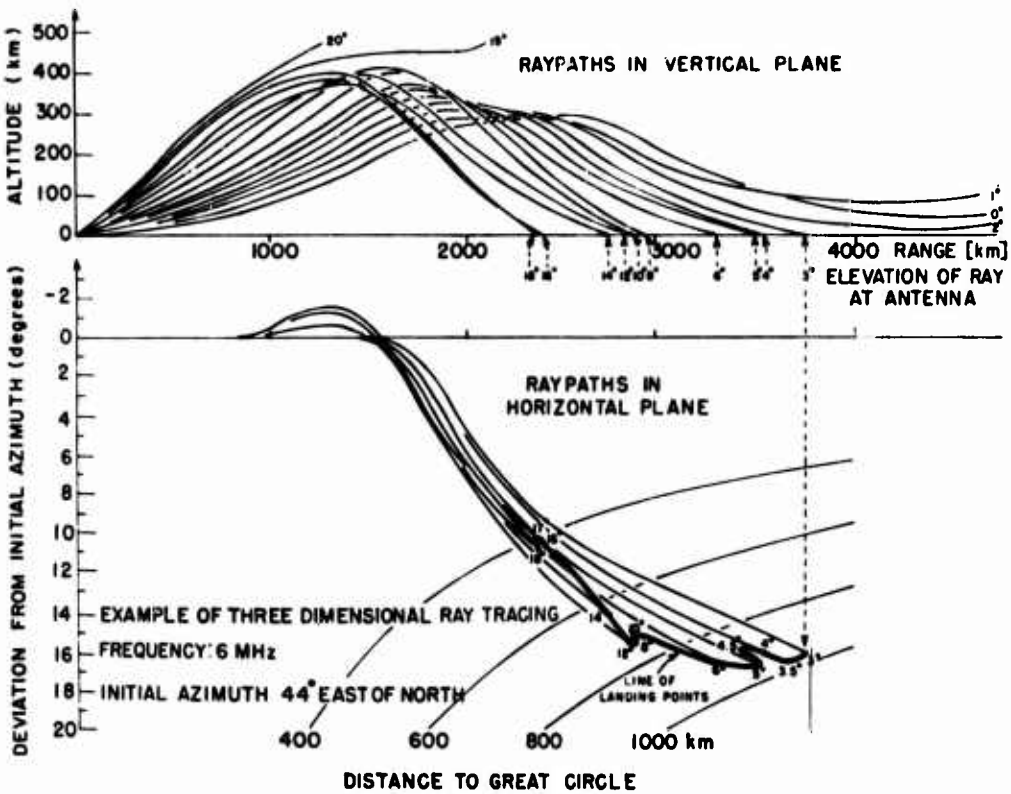

Figure 7. Example of Three-Dimensional Raytracing. Top shows projection of raypaths into the vertical plane of initial azimuth. Bottom shows projection into the horizontal plane

Figure 8 gives the results for 5 MHz. The numbers at the right ends of the loci of the landing points indicate the initial azimuth with respect to 45° east of north. The deviations are, as expected, mostly toward the south of the initial azimuth and are largest for the rays launched most northerly and are decreasing for rays intersecting less and less of the enhanced F region north of the trough wall. A test ray was launched at +13° azimuth so as to encounter only the rather horizontally stratified 2 MHz trough ionosphere. As expected, there were no deviations, and the range covered extended from 2200 to 3900 km, as indicated by the heavy line on the range axis. Landing points for rays -9° to -7° fall into two branches, the big looped curves resulting from rays leaving under low elevation angles (0° to 10°), and the long curves resulting from rays with elevation of 12° to 25°. Rays between 10° and 12° elevation are M-mode propagation,

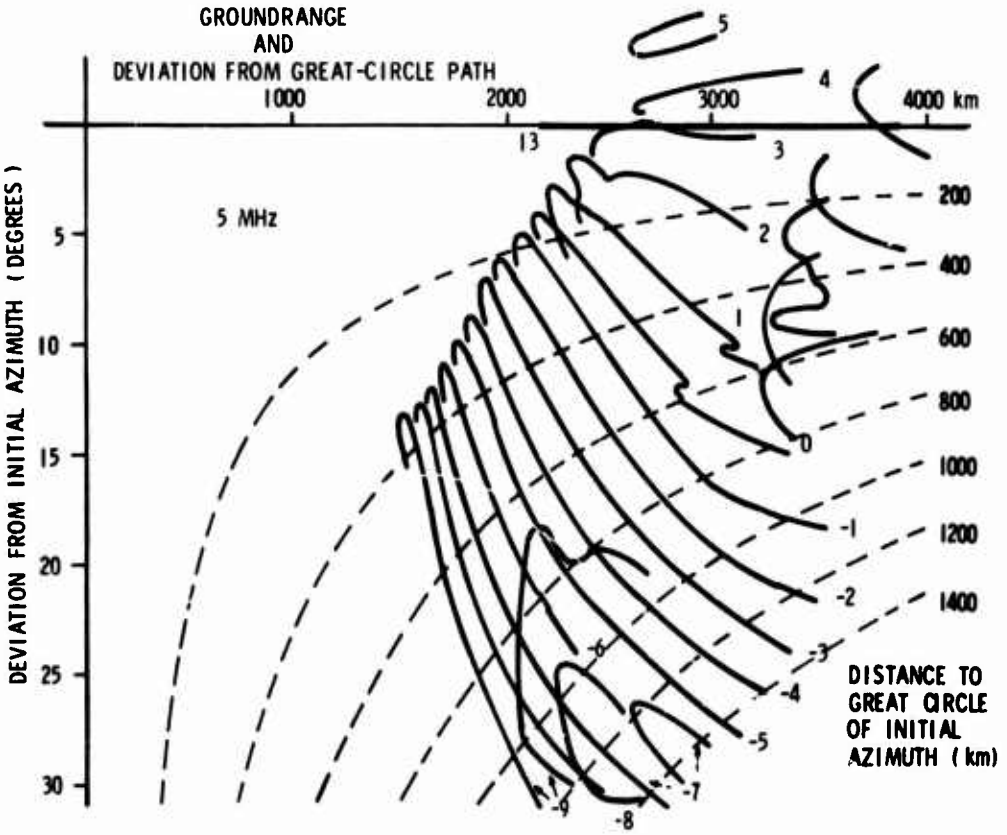

Figure 8. Raytracing Results for 5 MHz. Shown are the loci of the landing points as a function of the initial azimuths. Initial azimuths with respect to a central boresight of 45° east of north are indicated by the numbers to the right of the curves

skipping the earth due to ionospheric tilts at the reflection point. The skip distance can clearly be seen; the hooks at the upper ends of the landing-point curves result from the unfolding of the Pedersen ray in this diverging ionosphere. For rays -6° to -1°, all rays with elevations smaller than about 10° are M modes, the landing points for the higher rays forming a continuous curve. For azimuths 0° to 5°, low rays (0° to 5° elevation) reach the ground again, high rays (14° to 20° elevation) giving somewhat poor close-in coverage.

At 6 MHz (Figure 9), the situation is the same in general. The skip distance has increased, azimuths -9°, -8°, and -7° result again in two branches, one branch from low rays and a second branch from higher rays, the break being due to M-mode rays. Rays of -6° to -1° azimuth land only for elevations greater than about 5°. Rays of 0° to 5° azimuth have again a branch due to low elevations (about 0° to 8°), which at times are connected to the branch of higher elevations. The test ray propagated at 13° into the horizontally stratified trough shows no deviation and covers the range from 3100 to 4300 km.

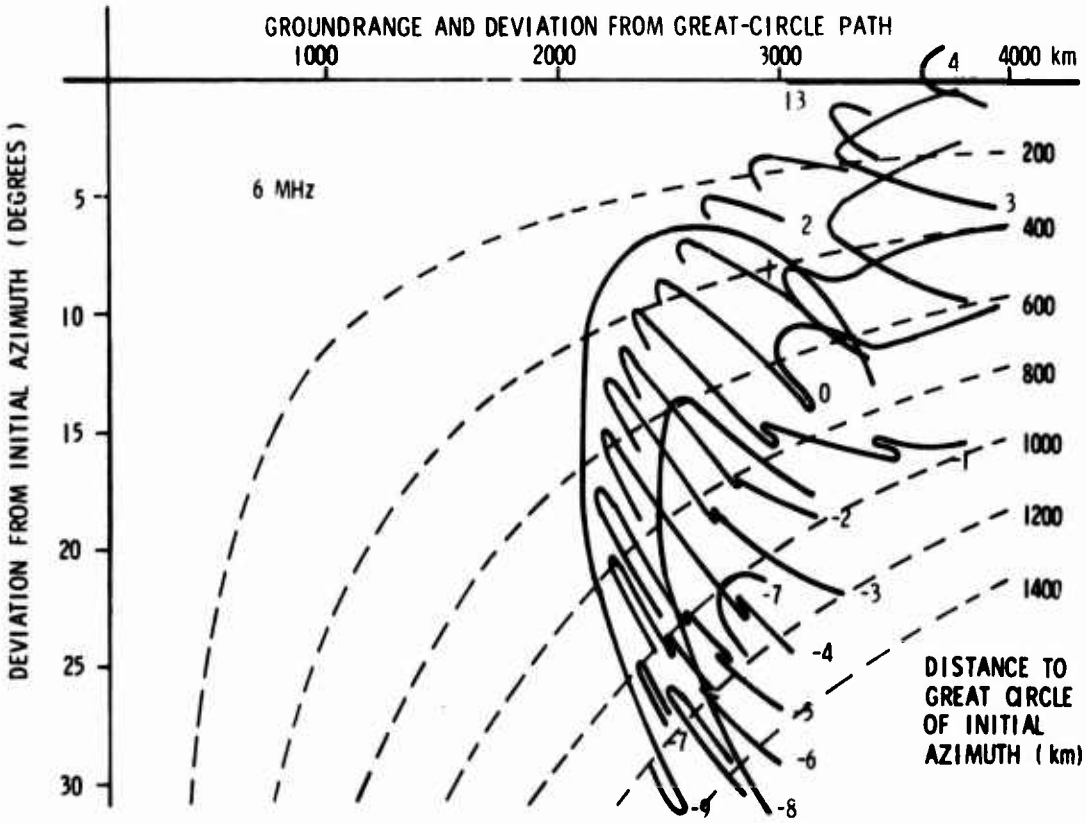

Figure 9. Raytracing Results for 6 MHz

Figure 10 shows the ground range and deviation for 7 MHz. Since this frequency is close to the MUF, high rays produce only broken-up coverage; for rays of -9° to -6° azimuth, the coverage is provided by low rays (0° to 5° elevation), with no high ray reaching the ground. The 2-MHz trough can no longer support propagation at this frequency.

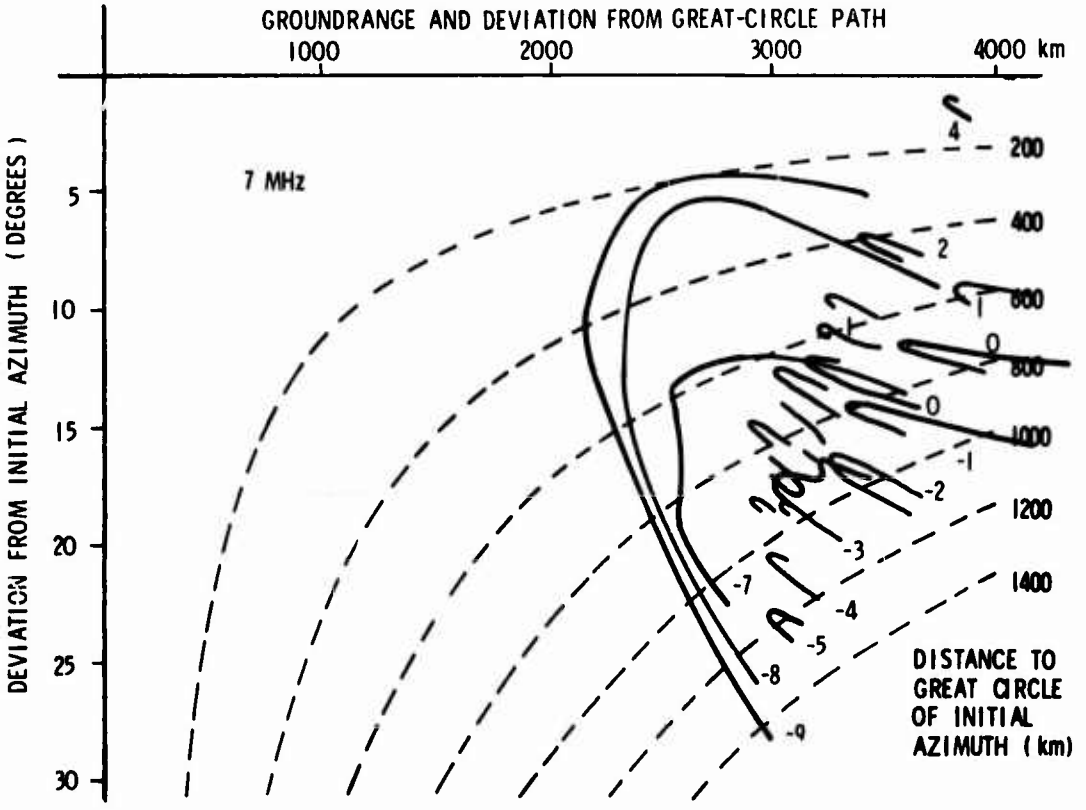

Figure 10. Raytracing Results for 7 MHz

The 8-MHz results (Figure 11) show that only rays of -9° to -6° azimuth are reflected, the deviation decreasing rapidly. The coverage is provided by elevation angles 0° to 5°. Finally, at 9 MHz (Figure 12), skip distance is almost 3000 km; only rays of -9° to -5° azimuth are reflected, relying on elevation angles $<5°$. For 10 MHz no reflection is achieved for the assumed initial azimuth of -9° to +13° with respect to 45° east of north.

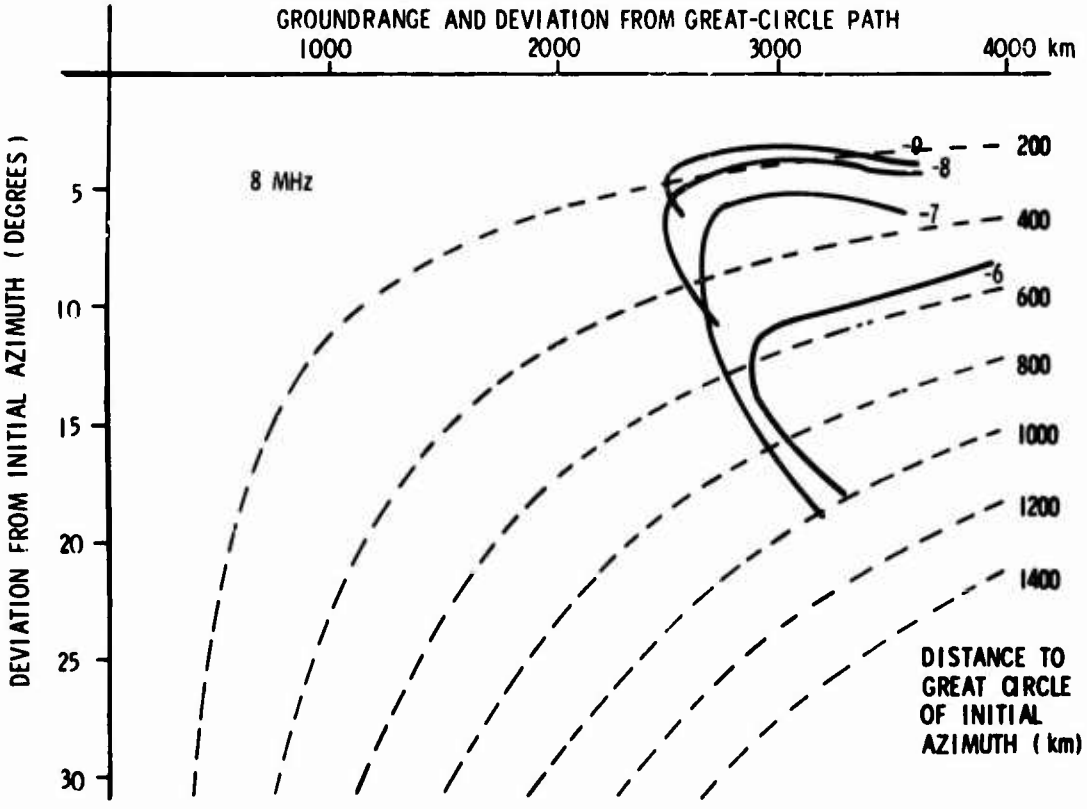

Figure 11. Raytracing Results for 8 MHz

6. CONCLUSIONS

The N_e-gradient at the poleward trough wall has been shown to severely affect the propagation of radio waves. Deviations from the original azimuth are shown to be as big as 25° or 1200 km off-great-circle for 5 and 6 MHz. For the rays landing at the skip distance, deviations are as big as 15° or 400 km off-great-circle. For 8 and 9 MHz the deviations are smaller, but only rays with low elevation angles propagate to the ground. It has to be pointed out, however, that the azimuths selected present the worst case as far as the deviation is concerned. Since the trough is a routinely occurring and variable feature of the southern edge of the polar ionosphere, an operational system requires instant calibration. This in turn requires either a large number of transponders or a real-time determination of the location of the trough together with a library of precalculated results from raypaths such as those shown here. A model of the arctic ionosphere and methods to determine the specifics in real time are being worked on at AFCRL.

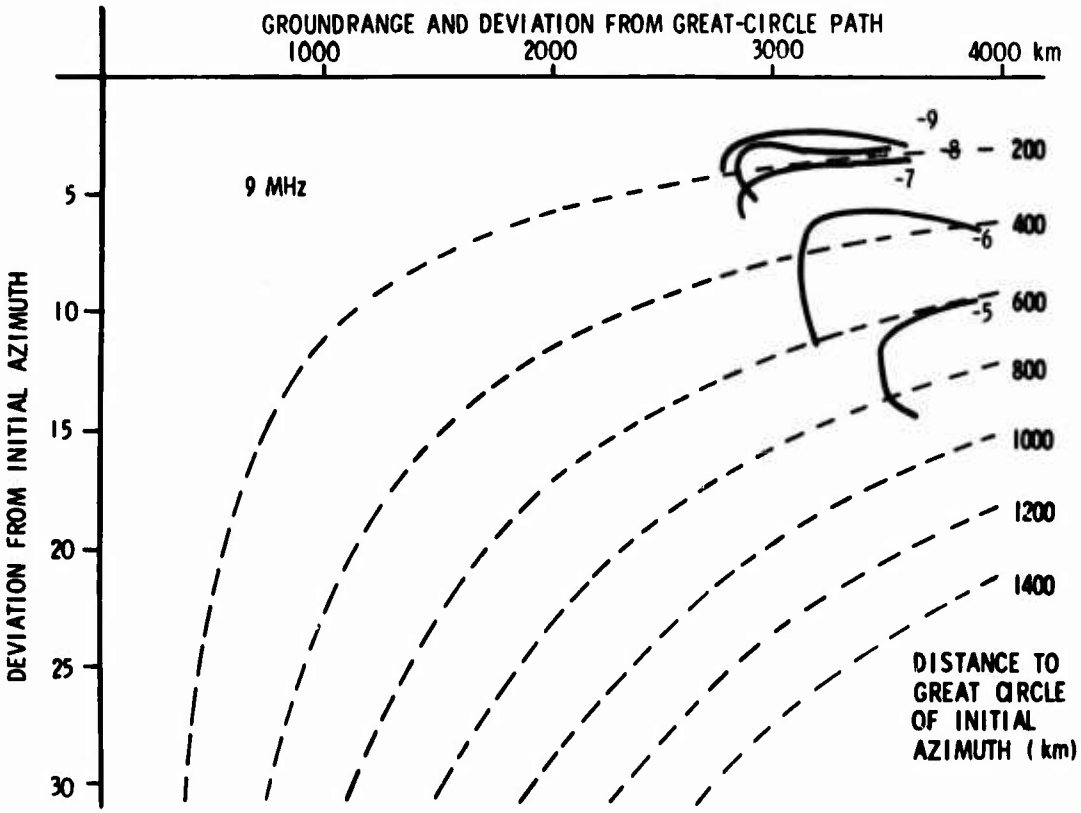

Figure 12. Raytracing Results for 9 MHz

The trough ionosphere supports propagation at 5 and 6 MHz with skip distances of 2000 to 3000 km, clearly demanding a high emphasis of the low-frequency capability of any system planned to operate in this region.

The deviations described result in double coverage of certain areas south of the trough wall and in regions not covered at all in the direction of the modeled beams.

It is planned to complete the computations for all azimuths, to determine total coverage possible for the available test case. POLAR FOX II data are available for 9 December 1971, and a comparison of the computer simulation and the actual data should show how well the modeling depicted the actual situation.

The computer program used allows the input of an arbitrary ionosphere rather than a mathematical model with all its shortcomings, and after the presently very high requirements on core memory have been reduced by proper use of disc storage it should be useful for producing a comprehensive library of results, or may even be used for real-time applications.

Finally, it should be pointed out that the demonstrated feasibility of calibrating an OTH radar field makes practical sense because a reasonably accurate description of the ionosphere now appears possible. Of particular aid are satellite pictures showing the large-scale extent of the aurora. These pictures are available from the AWS, and their use directly at the site or indirectly after AWS interpretation should be contemplated for any operational system. The interpretation of these pictures in terms of the corresponding ionospheric features has been achieved at AFCRL, and further refinement of the interpretation is underway.

References

1. Gassmann, G. J. (1972) An Ionospheric Model for the Arctic, Environmental Research Paper, No. 332, AFCRL-70-0562.
2. Gassmann, G. J. (1973) Analog Model 1972 of the Arctic Ionosphere, preprint, to be published as an AFCRL Report (February 1973).
3. Gassmann, G. J. (1972) High-latitude ionosphere, McGraw-Hill Yearbook of Science and Technology, McGraw-Hill Book Co., New York, pp. 257-260.
4. Wagner, R. A., and Pike, C. P. (1972) A discussion of arctic ionograms, AGARD Conf. Proc. 97, Frihagen, ed; pp. 4-1 to 4-20.
5. Muldrew, D. B. (1965) F-layer ionization troughs deduced from Alouette data, J. Geophys. Res. 70:2635-2650.
6. Andrews, M. K., and Thomas, J. O. (1969) Electron density distribution above the winter pole, Nature 221:223.
7. Pike, C. P. (1971) A latitudinal survey of the daytime polar F-layers, J. Geophys. Res. 76(No. 31):7745-7553.
8. Pike, C. P. (1972) Equatorward shift of the polar F-layer irregularity zone as a function of the Kp index, J. Geophys. Res. 77(No. 34):6911-6915.
9. Whalen, J. A., Buchau, J., and Wagner, R. A. (1971) Airborne ionospheric and optical measurements of noontime aurora, J. Atmos. Terr. Phys. 33 (No. 4):661-678.
10. Buchau, J., Gassman, G. J., Pike, C. P., Wagner, R. A., and Whalen, J. A. (1972) Precipitation patterns in the arctic ionosphere determined from airborne observations, Ann. Geophys. (Paris) 28(No. 2):443-453.
11. Hakura, Y. (1965) Tables and maps of geomagnetic coordinates corrected by the higher order spherical harmonic terms, Rep. Ionosph. Space Res. (Japan) 19:121-157.
12. Whalen, J. A. (1970) Auroral Oval Plotter and Nomograph for Determining Corrected Geomagnetic Local Time, Latitude, and Longitude in the Northern Hemisphere, AFCRL-70-0422, Environmental Research Paper No. 327, Bedford, Mass.

References

13. Evans, D. L. (1971) Comp., Ionospheric and tropospheric limitations to radar accuracy, Air Force Surveys in Geophysics, No. 231, AFCRL-71-0169.

14. Bowman, G. G. (1969) Ionization troughs below the F2-layer maximum, Planet. Space Sci. 17:777-796.

15. Buchau, J. (1972) Instantaneous versus averaged ionosphere, from "Arctic Ionosphere Modeling–Five Related Papers," Air Force Surveys in Geophysics, No. 241, AFCRL-72-0305.

16. Jones, R. M. (1968) A three-dimensional raytracing computer program, Radio Science 3(No. 1):93-94.

17. Wong, M. S. (1973) AFCRL Report to be published.